

(2)

AD-A264 722



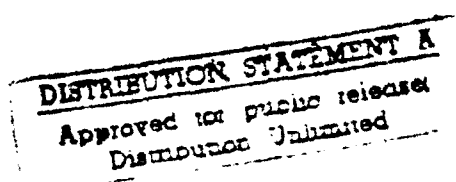
DTIC  
ELECTED  
MAY 20 1993  
**S C D**

---

Adaptive Airborne Radar Simulation  
with Equalization Filter Taps

M 93B0000041  
April 1993

B. N. Suresh Babu  
J. A. Torres



MITRE

Bedford, Massachusetts

93-11259



93 5 19 10 6

# REPORT DOCUMENTATION PAGE

Form Approved  
OMB No 0704-0188

Public reporting burden for this collection of information is estimated to average 1 hour per response, including the time for reviewing instructions, searching existing data sources, gathering and maintaining the data needed, and completing and reviewing the collection of information. Send comments regarding this burden estimate or any other aspect of this collection of information, including suggestions for reducing this burden, to Washington Headquarters Services, Directorate for Information Operations and Reports, 1215 Jefferson Davis Highway, Suite 1204, Arlington, VA 22202-4302, and to the Office of Management and Budget, Paperwork Reduction Project (0704-0188), Washington, DC 20503.

1. AGENCY USE ONLY (Leave blank)	2. REPORT DATE	3. REPORT TYPE AND DATES COVERED	
	April 1993		
4. TITLE AND SUBTITLE		5. FUNDING NUMBERS	
Adaptive Airborne Radar Simulation with Equalization Filter Taps			
6. AUTHOR(S)			
B. N. Suresh Babu J. A. Torres			
7. PERFORMING ORGANIZATION NAME(S) AND ADDRESS(ES)		8. PERFORMING ORGANIZATION REPORT NUMBER	
The MITRE Corporation 202 Burlington Road Bedford, MA 01730-1420		M 93B0000041	
9. SPONSORING/MONITORING AGENCY NAME(S) AND ADDRESS(ES)		10. SPONSORING/MONITORING AGENCY REPORT NUMBER	
The MITRE Corporation 202 Burlington Road Bedford, MA 01730-1420		M 93B0000041	
11. SUPPLEMENTARY NOTES			
12a. DISTRIBUTION/AVAILABILITY STATEMENT		12b. DISTRIBUTION CODE	
Approved for public release; distribution unlimited		A	
13. ABSTRACT (Maximum 200 words)			
<p>This document presents a reprint of a conference paper to be presented at the Summer Computer Simulation Conference (SCSC) in Boston, Massachusetts in July 1993. Adaptive nulling techniques are required to increase the tracking and detection of targets in the presence of jammers. Mitigating interference due to wideband, narrowband and multipath jamming may require additional temporal degrees of freedom. We have enhanced the capabilities of the advanced airborne radar simulation by incorporating additional temporal taps separated by a sampling rate interval (greater than Nyquist) into the conventional space time processing (STP) adaptive antenna architecture. This paper discusses the theory and implementation of STP using temporal filter taps, and presents three different examples illustrating the features of the simulation.</p>			
14. SUBJECT TERMS		15. NUMBER OF PAGES	
STP; radar; simulation; adaptive airborne radar		6	
		16. PRICE CODE	
17. SECURITY CLASSIFICATION OF REPORT		18. SECURITY CLASSIFICATION OF THIS PAGE	
Unclassified		Unclassified	
19. SECURITY CLASSIFICATION OF ABSTRACT		20. LIMITATION OF ABSTRACT	
Unclassified		None	

---

# Adaptive Airborne Radar Simulation with Equalization Filter Taps

M 93B0000041

April 1993

B. N. Suresh Babu  
J. A. Torres

5

Contract Sponsor MTC  
Contract No. N/A  
Project No. 021D  
Dept. D085

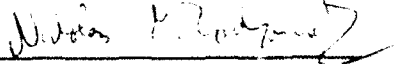
Approved for public release:  
distribution unlimited.

**MITRE**

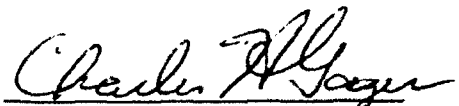
Bedford, Massachusetts

Accesision For	
NTIS	CRA&I <input checked="" type="checkbox"/>
DTIC	TAB <input type="checkbox"/>
Unannounced <input type="checkbox"/>	
Justification	
By _____	
Distribution /	
Availability Codes	
Dist	Avail and/or Special
A-1	

Department Approval:

  
Nicholas M. Tomljanovich

MITRE Project Approval:

  
Charles H. Gager

## PREFACE

This document presents a reprint of a conference paper to be presented at the Summer Computer Simulation Conference (SCSC) in Boston, Massachusetts in July 1993. Adaptive nulling techniques are required to increase the tracking and detection of targets in the presence of jammers. Mitigating interference due to wideband, narrowband and multipath jamming may require additional temporal degrees of freedom. We have enhanced the capabilities of the advanced airborne radar simulation by incorporating additional temporal taps separated by a sampling rate interval (greater than Nyquist) into the conventional space time processing (STP) adaptive antenna architecture. This paper discusses the theory and implementation of STP using temporal filter taps, and presents three different examples illustrating the features of the simulation.

## ADAPTIVE AIRBORNE RADAR SIMULATION WITH EQUALIZATION FILTER TAPS

B. N. Suresh Babu and J. A. Torres  
The MITRE Corporation  
202 Burlington Road  
Bedford, Massachusetts 01730-1420

### ABSTRACT

Space-time processing (STP) provides an adaptive filter for an airborne phased-array radar to detect targets in clutter and jamming that have spatial and Doppler spread. We developed a flexible airborne radar simulation to identify limitations in the techniques and to evaluate the capabilities of different STP designs. One of the space-time architectures, jointly adaptive STP in the element space, employs joint processing of array elements and pulse train data. The array elements provide the azimuth (spatial) information, and the pulse repetition interval (PRI) taps or pulses provide the Doppler information required to form the two-dimensional azimuth-Doppler filter. In the adaptive mode, additional temporal information from taps separated by a sampling rate interval (greater than Nyquist) provide additional degrees of freedom to mitigate interference due to wideband, narrowband, and multipath jamming. This paper discusses the theory and implementation of STP using temporal equalization filter taps, and presents three different examples illustrating the features of the simulation.

### INTRODUCTION

New surveillance radars for strategic and tactical applications are needed to detect targets with very low cross sections. This requires a large power-aperture product which, in turn, increases the level of the clutter and jammer signals received from the antenna sidelobe region. Receiving antennas with ultra-low sidelobe patterns and adaptive sidelobe cancellers have been proposed for large phased-array radars to suppress these interference signals. However, MITRE identified limitations in these techniques for achieving the required interference signal suppression, and developed a flexible simulation to evaluate the capabilities of proposed STP designs.

In a previously published paper (Suresh Babu and Torres 1992), we describe the features of a simulation tool which enables us to evaluate advanced airborne radars with adaptive antenna techniques (STP). Figure 1 shows the global features of the airborne radar simulation using these techniques. The software calculates radar performance in jamming and clutter scenarios and models three different STP designs (i.e., element space, beam space, and

subarraying) for both jamming and clutter suppression. STP, the adaptive joint processing of pulse train and array element, beam, or subarray data, adaptively reduces the jamming and sidelobe clutter to enhance detectability of targets. The conventional STP filter is formed by placing a tapped delay line at the output of each element, beam, or subarray of the antenna array, with the taps spaced by one pulse repetition interval (PRI), wherein the degrees of freedom are equal to the number of pulses times the number of elements, beams, or subarrays. Adaptive weights for each of these taps are derived based on assumptions made about the different spatial and Doppler correlation properties of the target, clutter, noise, and jamming.

Adaptive nulling techniques are required to increase the tracking and detection of targets in the presence of jammers. Mitigating interference due to wideband and narrowband jamming may require additional temporal degrees of freedom. One possible approach is to incorporate additional temporal taps separated by a sampling rate interval (greater than Nyquist) into the conventional STP architecture, as shown in figure 2. In addition, these taps can provide temporal information to also mitigate the effects of multipath jamming. This paper discusses the theory and implementation of STP with temporal equalization filter taps which are an integral part of the adaptive weight computation, wherein the degrees of freedom are equal to the number of taps times the number of pulses times the number of elements, beams, or subarrays.

The temporal correlation differences between the received noise, target, and jamming signals at the temporal filter taps are used to compensate for narrowband, wideband, and multipath jamming. The degree of performance improvement achievable with these filter taps is dependent on the temporal correlation properties of the received signals, the number of filter taps, and the short delays between the taps. This simulation enables design engineers to perform complexity versus performance trade-off studies.

### CORRELATION PROPERTIES OF RECEIVED SIGNALS

We differentiate between narrowband and wideband jamming based on the jammer bandwidth relative to the

radar receiver bandwidth. For narrowband jamming, the jammer bandwidth is less than the radar bandwidth. However, for wideband jamming, it is significantly greater. Following pulse compression (i.e., matched filtering), the wideband jammer bandwidth is limited by the radar receiver. The correlation properties of the wideband and narrowband jamming are different from each other and also from the target, as discussed below.

The spatial correlation properties of the received signals at the antenna elements are based on the element-to-element path delay differences related to their spatial locations. However, the noise is spatially uncorrelated from element-to-element. The temporal correlation properties of the received signals are based on the spectrum of the received signals and the matched filter response. For the analysis, we assume that the radar transmits a pulse train with linear frequency modulation (chirp) and employs matched filtering (pulse compression) on receive. Figure 3 illustrates the matched filter response of a chirp signal with high pulse compression (Wehner 1987) which is bandlimited to  $\pm(B/2)$ , where  $B$  is the radar bandwidth. Prior to matched filtering, the wideband jammer and noise have flat input spectrums over all frequencies ranging from  $-(f_s/2)$  to  $(f_s/2)$ , where  $f_s$  is the sampling rate. Following matched filtering, the output spectrums of these signals are controlled by both the passband and stopband characteristics of the matched filter response and become bandlimited to  $\pm(B/2)$ . For the analysis, the input spectrum of the narrowband jammer is assumed to be flat and bandlimited to  $\pm(B_J/2)$  with no sidelobes (i.e., ideally rectangular), where  $B_J$  is the bandwidth of the jammer and is assumed to be, at most, the radar bandwidth  $B$ . The output spectrum of the narrowband jammer is controlled only by the passband of the matched filter response. Therefore, the output spectrums of a wideband jammer and noise are different from that of a narrowband jammer. Note that even in the limit of  $B_J = B$ , the wideband and narrowband jamming output spectrums are not identical due to the stopband characteristics of the matched filter response. Consequently, the temporal correlation functions for these signals are different.

The temporal correlation function and its power spectral density are Fourier transform pairs; the correlation functions are derived by taking the inverse Fourier transform of the output spectrum for the different signals. The temporal correlation properties of these signals are modeled as a sinc function due to their flat bandlimited spectrums with matched filtering. The steady-state covariance matrices for the received signals are based on the spatial and temporal correlation functions listed in table 1. Each entry of a signal covariance matrix corresponds to the correlation functions evaluated at different antenna elements, pulses, and taps. Table 1

shows the differences in the spatial and temporal correlation functions for the noise, target, and narrowband and wideband jamming received signals. For conciseness, the mathematical details of the models are not described, and the spatial and temporal cross terms have been omitted from the expressions.

#### Adaptive Weight Computation

The adaptive weights are computed by multiplying the sum of the covariance matrices for the noise, clutter, and jamming with a steering vector. The covariance matrices are constructed based on the spatial and temporal correlation properties of the received signals. The steering vector (Brennan and Reed 1973) is tuned for a hypothesized target with specified spatial and temporal correlation properties.

#### RESULTS

We present three examples (with jamming interference only and with no clutter) to illustrate various features of the simulation related to the adaptive temporal filter. In these examples, only a single PRI tap (pulse) is processed, and the target is assumed to be located at the peak of the mainlobe. The first example illustrates the mitigation of wideband multiple noise-like jammers (eight) located in the sidelobes of an array with temporal taps. The second and third examples illustrate that mainlobe narrowband jamming and multipath jamming can be mitigated by the additional temporal taps. For conciseness, the specific parameters and performance measures for all of the examples are included in the figures. Note that the adapted signal-to-interference ratio (SIR) is normalized by the quiescent signal-to-noise ratio (SNR) so that the performance measures are invariant of target power.

#### Example 1

This example illustrates the effect of additional temporal filter taps in the STP architecture on the nulling capability of multiple wideband jammers (eight) located in the sidelobes of a 15-element linear array. Table 1 shows that a target can be spatially discriminated from a wideband jammer located in the antenna sidelobes due to the different spatial correlation properties between the target and the jammer. Figure 4 presents a plot of normalized eigenvalues of the spatial jammer-plus-noise covariance matrix for three different radar bandwidths. As the radar bandwidth increases, the number of required spatial degrees of freedom increases due to the  $\pi B T_J (e_1 - e_2)$  spatial correlation term shown in table 1. Since the system has only 15 spatial degrees of freedom, it causes degradation in performance (normalized adapted SIR), as shown by the solid curve in figure 4. Ideally, increasing the number of

spatial degrees of freedom (i.e., more antenna elements) can completely mitigate the wideband jammers. However, if the number of spatial degrees of freedom is limited, additional temporal taps can be used to discriminate between the differences in correlation properties of the target and wideband jamming received signals (White 1983). Figure 5 compares the nulling performance of an adaptive array with two, four, and six temporal filter taps. The signals are sampled at a higher rate (two and one-half times the Nyquist rate) to take advantage of the temporal correlation properties of the received signals. This figure illustrates that additional temporal degrees of freedom mitigate the reduction in performance due to wideband jamming.

#### Example 2

This example illustrates the mitigation of a narrowband jammer located at the peak of the mainlobe using temporal taps. In table 1, note that a wideband jammer located at the peak of the mainlobe cannot be spatially discriminated from a target or temporally discriminated from noise due to the equivalent correlation properties. Although a mainlobe narrowband jammer cannot be spatially discriminated from a target, it can be temporally discriminated from noise. Figure 6 compares the nulling performance of an adaptive array with two, four, six, and eight temporal taps. Note that the tap spacing is small due to oversampling (two and one-half times the Nyquist rate). As shown, additional temporal degrees of freedom mitigate the effects of a mainlobe narrowband jammer.

#### Example 3

The first two examples illustrate that temporal taps mitigate the effects of direct jamming with no multipath. However, these taps can also mitigate multipath jamming that is scattered off the earth's surface. The scattered jamming signals arrive at the radar from different spatial directions with different temporal delays. Although the direct jamming signals are in the sidelobes, multipath jamming signals can be distributed throughout the mainlobe. As shown in another study (Barile, et al. 1993), the mitigation of multipath jamming is based on a high degree of correlation among the scattered jamming signals. This example illustrates the feature of the simulation that allows us to read in a covariance matrix from an output file. The covariance matrix is constructed based on the above referenced multipath jamming model. The direct wideband jammer is located in the sidelobes of a 16-element linear array. Multipath jamming signals (i.e., 48) are distributed throughout the mainlobe and the first sidelobe. Note that the tap spacing is based on two and one-half times oversampling to take advantage of the temporal correlation of each multipath jamming signal. Figure 7 illustrates the performance improvement

resulting from using temporal taps to mitigate multipath jamming.

#### SUMMARY

The flexible simulation tool described in this paper allows system engineers to evaluate the performance of STP techniques with temporal equalization filters for narrowband, wideband, and multipath jamming suppression. The software incorporates the additional temporal weights as an integral part of the adaptive weight computation employing either the element space, beam space, or subarraying architecture. The examples presented illustrate the features of the simulation used to perform complexity versus performance trade-offs by varying the number of temporal taps (i.e., degrees of freedom) and the spacing between them.

#### LIST OF REFERENCES

1. Suresh Babu, B.N. and J.A. Torres. 1992. "Airborne Radar Simulation with Adaptive Antenna Techniques." Summer Computer Simulation Conference.
2. Wehner, D.R. 1987. *High Resolution Radar*. Artech House, Norwood, Massachusetts.
3. Brennan, L.E. and I.S. Reed. 1973. "Theory of Adaptive Radar." *IEEE Transactions on Aerospace and Electronic Systems*, AES-9.
4. White, W.D. 1983. "Wideband Interference Cancellation in Adaptive Sidelobe Cancellers." *IEEE Transactions on Aerospace and Electronic Systems*, AES-19.
5. Barile, E.C.; R.L. Fante; T.P. Guella; and J.A. Torres. 1993. "Performance of Space-Time Adaptive Airborne Radar." IEEE National Radar Conference.

Table 1. Differences in Correlation Functions of Received Signals

Received Signal	Spatial	Temporal	Definitions	Remarks
Noise	$\delta(\epsilon_1 - \epsilon_2)$	$e^{j\pi B(\ell_1 - \ell_2)\tau} \cdot e^{-j\frac{\pi B}{\tau_u}((\ell_1 - \ell_2)\tau)^2}$ $\cdot \text{sinc}\{\pi B(\ell_1 - \ell_2)\tau\} \cdot \delta(k_1 - k_2)$	$\epsilon_i = \text{element indices}$ $\ell_i = \text{temporal tap indices}$ $k_i = \text{pulse indices}$ $\delta = \text{Kronecker delta function}$ $B = \text{radar bandwidth}$ $\tau_u = \text{uncompressed pulsewidth}$ $\tau = \text{tap spacing}$	<ul style="list-style-type: none"> <li>Uncorrelated from element-to-element</li> <li>Sinc type of temporal correlation with quadratic phase and uncorrelated from pulse-to-pulse</li> </ul>
Wideband Jammer	$e^{j\omega_c T_j(\epsilon_1 - \epsilon_2)}$ where, $T_j = \frac{\Delta}{c} \sin \theta_j$	Noise-like, except for an additional spatial term resulting in the following replacement: $(\ell_1 - \ell_2)\tau \rightarrow (\ell_1 - \ell_2)\tau + T_j(\epsilon_1 - \epsilon_2)$	$\theta_j = \text{jammer azimuth}$ $T_j = \text{jammer element-to-element delay}$ $\omega_c = \text{radar center frequency}$ $\Delta = \text{element spacing}$ $c = \text{speed of light}$	<ul style="list-style-type: none"> <li>Linear phase front across elements</li> <li>Spatial discrimination from target and noise</li> <li>Noise-like temporal correlation and uncorrelated from pulse-to-pulse</li> </ul>
Narrowband Jammer	Same as wideband jammer	$e^{j\omega_c \beta[(\ell_1 - \ell_2)\tau + (k_1 - k_2)T]}$ $\cdot \text{sinc}\{\pi B_j[(\ell_1 - \ell_2)\tau + (k_1 - k_2)T]\}$	$B_j = \text{jammer bandwidth}$ $T = \text{pulse spacing (PRD)}$ $\beta_j = \text{jammer Doppler}$	<ul style="list-style-type: none"> <li>Spatial discrimination from target and noise</li> <li>Sinc type of temporal correlation with linear phase and pulse-to-pulse correlation</li> <li>Temporal discrimination from noise and target</li> </ul>
Target	$e^{j\omega_c T_s(\epsilon_1 - \epsilon_2)}$ where, $T_s = \frac{\Delta}{c} \sin \theta_s$	$e^{j\omega_c \beta_s(k_1 - k_2)T} \cdot e^{j\pi B(\ell_1 - \ell_2)\tau}$ $\cdot \text{sinc}\{\pi B(\ell_1 - 1)\tau\} \cdot \text{sinc}\{\pi B(\ell_2 - 1)\tau\}$	$T_s = \text{target element-to-element delay}$ $\beta_s = \text{target Doppler}$ $\theta_s = \text{target azimuth}$	<ul style="list-style-type: none"> <li>Spatial and pulse-to-pulse (Doppler) discrimination from noise and jamming</li> </ul>

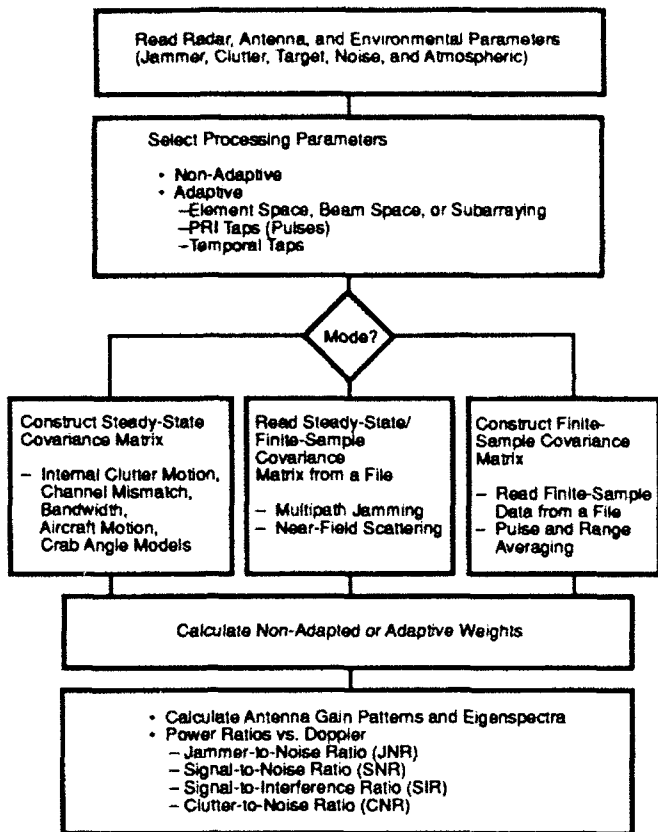


Figure 1. Global Features of Airborne Radar Simulation

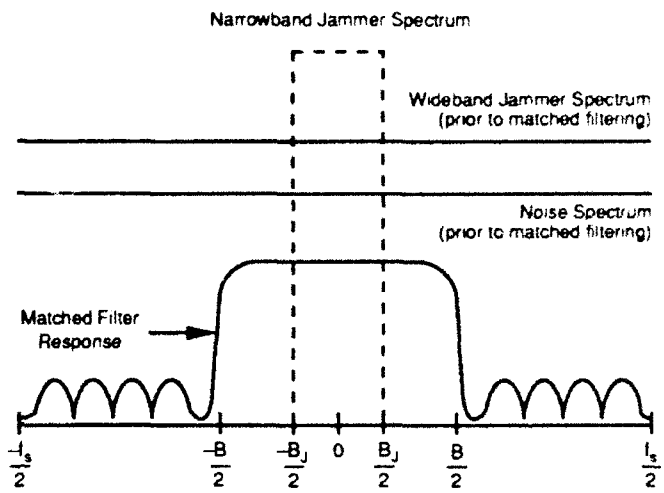
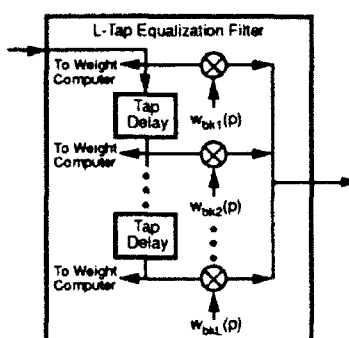
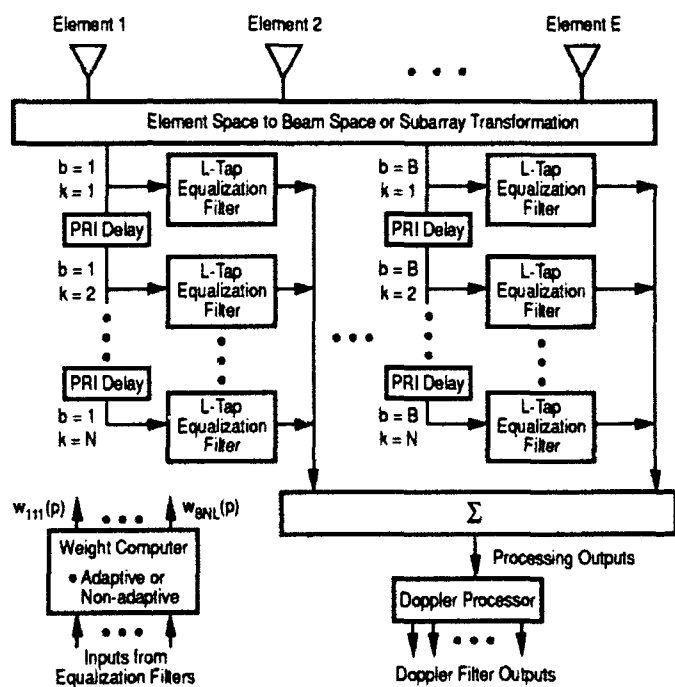


Figure 3. Illustration of Received Signal Spectrums and Matched Filter Response



E = Number of elements  
 B = Number of beams, subarrays, or elements  
 N = Number of pulses (processing order)  
 L = Number of temporal taps  
 b = Beams, subarrays, or elements index  
 k = Pulse index  
 p = Processing output index  
 Number of degrees of freedom =  $B \times N \times L$

Figure 2. Adaptive Processing Architecture with Temporal Taps

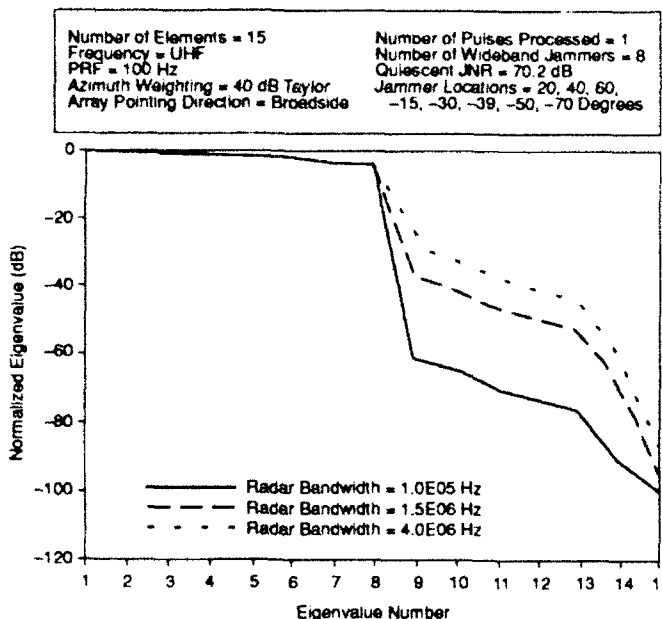


Figure 4. Effect of Radar Bandwidth on Spatial Jammer-Plus-Noise Eigenvalues

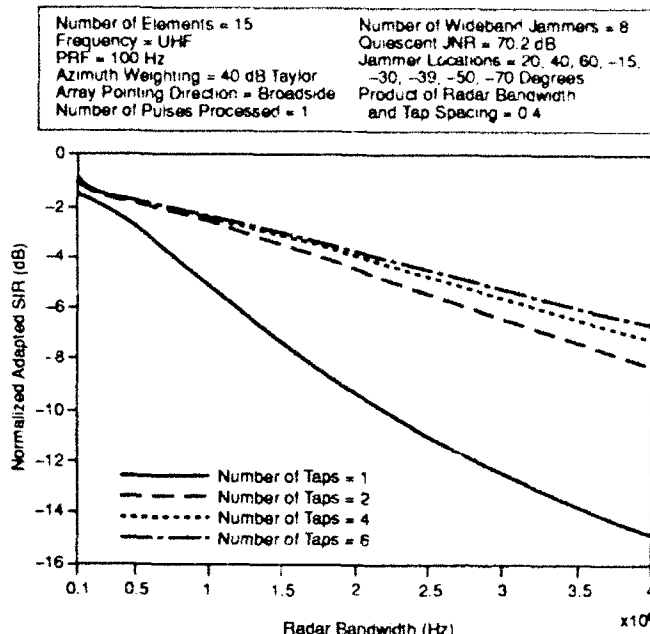


Figure 5. Mitigation of Sidelobe Wideband Jamming with Temporal Taps

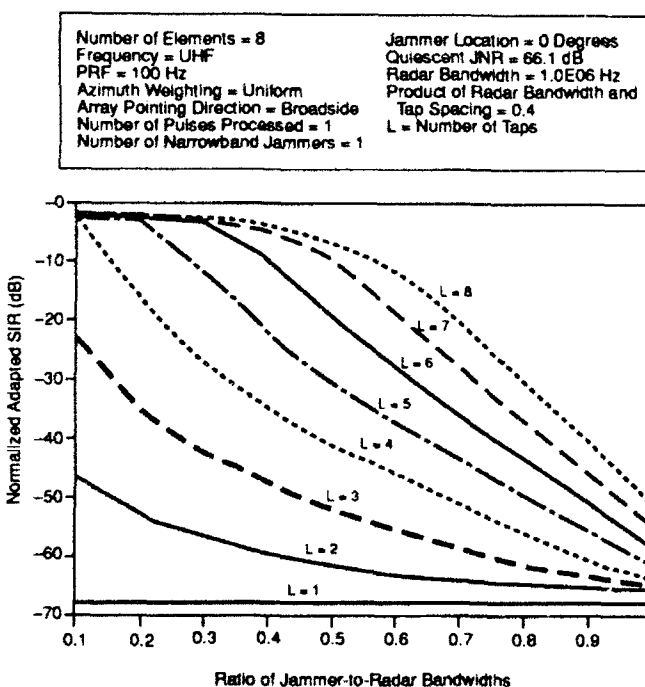


Figure 6. Cancellation of a Mainlobe Narrowband Jammer with Temporal Taps

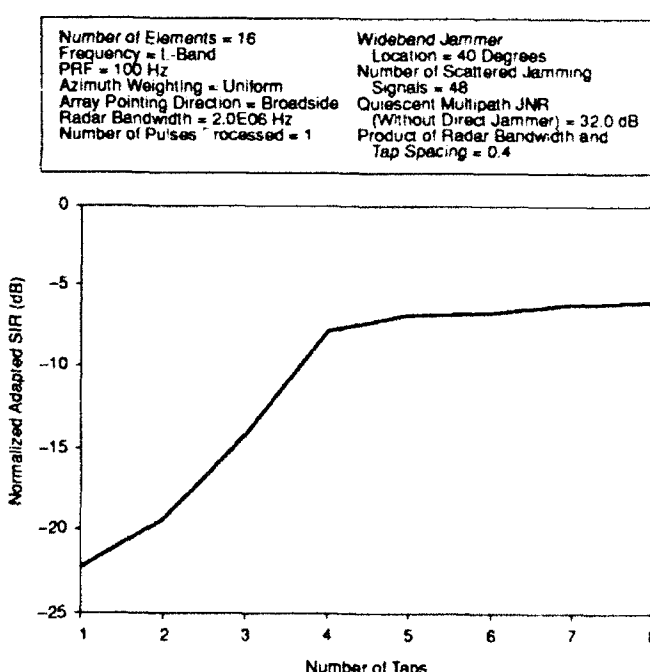


Figure 7. Performance Comparison of Multipath Jamming Mitigation with Temporal Taps